Human Molecular Genetics, 2016, Vol. 25, No. 9 1690–1702

doi: 10.1093/hmg/ddw038
Advance Access Publication Date: 16 February 2016
Original Article

ORIGINAL ARTICLE

Acute and crucial requirement for MeCP2 function upon transition from early to late adult stages of brain maturation

Fang Du[1,†], Minh Vu Chuong Nguyen[1,‡], Ariel Karten[1], Christy A. Felice[1], Gail Mandel[2] and Nurit Ballas[1,*]

[1]Department of Biochemistry and Cell Biology, Stony Brook University, Stony Brook, NY 11794, USA and [2]Vollum Institute, Howard Hughes Medical Institute, Oregon Health and Science University, Portland, OR 97239, USA

*To whom correspondence should be addressed. Tel: +1 631 632 1572; Fax: +1 631 632 8575; Email: nurit.ballas@stonybrook.edu

Abstract

Germline mutations in the X-linked gene, methyl-CpG-binding protein 2 (MECP2), underlie most cases of Rett syndrome (RTT), an autism spectrum disorder affecting approximately one in 10 000 female live births. The disease is characterized in affected girls by a latent appearance of symptoms between 12 and 18 months of age while boys usually die before the age of two. The nature of the latency is not known, but RTT-like phenotypes are recapitulated in mouse models, even when MeCP2 is removed at different postnatal stages, including juvenile and adolescent stages. Unexpectedly, here, we show that within a very brief developmental window, between 10 (adolescent) and 15 (adult) weeks after birth, symptom initiation and progression upon removal of MeCP2 in male mice transitions from 3 to 4 months to only several days, followed by lethality. We further show that this accelerated development of RTT phenotype and lethality occur at the transition to adult stage (15 weeks of age) and persists thereafter. Importantly, within this abbreviated time frame of days, the brain acquires dramatic anatomical, cellular and molecular abnormalities, typical of classical RTT. This study reveals a new postnatal developmental stage, which coincides with full-brain maturation, where the structure/function of the brain is extremely sensitive to levels of MeCP2 and loss of MeCP2 leads to precipitous collapse of the neuronal networks and incompatibility with life within days.

The X-linked methyl-CpG-binding protein 2 (*MECP2*) gene is expressed globally, yet its loss-of-function, caused by germline mutations, is most notable in the brain and manifests primarily as Rett syndrome (RTT) (1,2). Girls born with mutations in *MECP2* develop normally for ~12–18 months and then start to regress, losing purposeful hand motions and speech and developing several autistic-like features, including repetitive behaviors, social withdrawal and expressionless face. Cognitive deficits, motor abnormalities and numerous other neurological problems become apparent at later times (3,4). The impact of MeCP2 loss on brain anatomy and function is supported by several studies indicating that RTT patients and mouse models have reduced brain size, increased neuronal cell density, reduced nuclear size, reduced dendritic arborization and spine density (1,5–9), and impaired synaptic transmission and plasticity (10–14).

Several recent studies, including our own, have shown that inducible loss of MeCP2 in mice, even at an early adult stage, results in severe manifestation of RTT-like phenotypes followed by lethality, similar to mice with germline mutations in *Mecp2* (15–17). Importantly, our study showed that inducible loss of MeCP2 at juvenile stage, which coincides with the onset of classic RTT, and early adult stage, manifested in similar kinetics of

†Present address: Department of Pharmacology and Toxicology, Kansas University School of Pharmacology, Kansas.
‡Present address: GREPI-UGA EA7408, Université Grenoble Alpes, Grenoble, France.
Received and Revised: January 15, 2016. **Accepted:** February 5, 2016

symptom initiation and progression (15). Furthermore, in both developmental stages, the brain acquired similar abnormalities including global shrinkage of the brain, which resulted in higher than normal neuronal cell density, severely retracted mature dendritic arbor structures and significant reduction in the levels of specific synaptic proteins (15).

Here, we characterized stereotypical brain features at more advanced adult stages, when the brain reaches maturation by these criteria, and analyzed the impact of MeCP2 loss at these stages. Unexpectedly, we find that in addition to the classical onset of RTT at ~5 weeks of age in male mice with germline deletion, and in mice where MeCP2 loss was induced at 5 weeks of age, there is another highly critical MeCP2-sensitive stage at 15 weeks of age. Whereas the manifestation of severe RTT-like symptoms upon inducible loss of MeCP2 at 5 or even 10 weeks of age in males ranged between 10 and 18 weeks of removal of MeCP2, with a median survival time of 16–17 weeks, inducible loss of MeCP2 at 15 weeks of age or later resulted in accelerated symptom progression and lethality with a median survival time of only 4–7 days. Within this compressed time frame, the brain acquired anatomical, cellular and molecular abnormalities similar and perhaps more severe than at earlier stages. Our results suggest that there is acute and highly critical requirement for MeCP2 as the neuronal networks become increasingly complex and the brain reaches full maturation.

Results

Depletion of MeCP2 in adult mice induces rapid onset of RTT-like symptoms followed by lethality within only few days

According to recent criteria [e.g. (18)], we have defined mouse postnatal developmental stages as juvenile (3–6 weeks), adolescent (6–14 weeks) and adult (14 weeks and beyond). Our previous study showed that the elimination of MeCP2 in juvenile (5-week-old) or adolescent (early adult) mice (10 weeks old) leads to a broad range of RTT-like symptoms including brain abnormalities, such as shrinkage of the brain, increased neuronal density, retraction of dendritic arbor structures and eventually death (15) with 50% survival at 16–17 weeks. Because the brain continues to mature beyond this time interval (19,20), we sought to test for effects of removing MeCP2 in advanced adult stages using the tamoxifen (Tam)-inducible CreER and the *Mecp2*^{loxJ} (1) mouse lines. Unless otherwise stated, *Mecp2*$^{loxJ/y}$*/CreER* male mice were injected with Tam for 7 consecutive days as we previously described (15) and analyzed with time for overall health, starting from the last Tam injection. We first analyzed the consequences of MeCP2 removal in 48-week-old mice (48W), when mice are still within their late reproductive period. To our surprise, and contrary to 5 W- or 10 W-Tam-injected mice, the 48 W-Tam-injected *Mecp2*$^{loxJ/y}$*/CreER* males had a very short life span, with 50% survival at ~7 days post the last Tam injection (Fig. 1A). The extremely rapid death is not due to toxicity of the Tam injection because none of the control littermates (WT, *CreER* and *Mecp2*$^{loxJ/y}$) injected similarly with Tam died during the period analyzed or at any time later (Fig.1A and data not shown). To determine whether the rapid lethality observed with the 48 W-Tam-injected *Mecp2*$^{loxJ/y}$*/CreER* male mice was due to RTT-like symptom onset rather than sudden death from other unrelated health issues, we evaluated daily the kinetics of the appearance of overt RTT-like symptoms. We used the observational phenotypic scoring system (0–10) described previously (15) for five typical phenotypes: mobility, gait, hind limb clasping, tremors and general condition. Our results show that the 48 W-Tam-injected *Mecp2*$^{loxJ/y}$*/CreER* male mice developed progressive RTT-like phenotypes; however, unlike the 5- and 10-week-old Tam-injected mice which reached a score of 6–7 at 18 weeks from injection (15), the kinetics of symptom development was extremely rapid, reaching an aggregate score of 6–7 within 6–8 days from the last Tam injection (Fig. 1B). All control age-matched male littermates (Tam-injected WT, *CreER*, and *Mecp2*$^{loxJ/y}$ and Veh-injected *Mecp2*$^{loxJ/y}$*/CreER*) remained equally healthy (Fig. 1B).

Because our data show remarkable differences in the rate of initiation and progression of symptoms as well as in lethality between the loss of MeCP2 at 10 and 48 weeks of age, we first sought to more precisely determine the boundaries of this window as well as to exclude the possibility that the observed phenotype was related to aging. To this end, we analyzed *Mecp2*$^{loxJ/y}$*/CreER* male mice injected with Tam at 20 and 34 weeks of age. Similar to the 48-week-old mice, the loss of MeCP2 in both, 34- and 20-week-old mice, resulted in severe RTT-like symptoms, reaching a score of 6–8 within 5–6 days post-injection followed by premature death with 50% survival at 6 and 4 days post-injection, respectively (Supplementary Material, Fig. S1A–D). We next moved down to 15-week-old (15 W) *Mecp2*$^{loxJ/y}$*/CreER* mice. Remarkably, these mice also developed rapid RTT-like symptoms followed by lethality with 50% survival at 7 days, just like the 48-, 34- and 20-week-old mice (Fig. 1C and D), although some mice survived up to 12–18 days post-injection, while none of the 48-, 34- or 20-week-old mice injected with Tam, survived past 10 days from injection (Fig. 1A–D and Supplementary Material, Fig. S1A–D). In contrast to these mice, all of the age-matched control littermates remained healthy during the period analyzed (Fig. 1A–D and Supplementary Material, Fig. S1A–D) and far beyond unless they were sacrificed (data not shown).

To exclude the possibility that different Tam preparations might contribute to such differential rates in symptom initiation and progression within this short interval between 10 and 15 weeks of age, we injected 10-week-old *Mecp2*$^{loxJ/y}$*/CreER* mice in parallel with 15-week-old mice, using the same Tam preparation, and confirmed the slow (Fig. 1E and F) versus rapid (Fig. 1C and D) kinetics of symptom progression and survival, respectively. Specifically, and supporting our previous studies (15), the 10-week-old mice reached a score of 3 within 4 weeks from injection and none of them died within this period, whereas the 15-week-old mice reached a score of 8 within 2 weeks and none of them survived past 3 weeks (Fig. 1G and H). Furthermore, to eliminate the possibility that the rapid depletion of MeCP2 specifically at 15 weeks of age caused the sudden symptoms, we injected 15-week-old mice for 14 days with half the amount of Tam (50 mg/kg body weight) rather than for 7 days with the full amount (100 mg/kg body weight). These mice developed symptoms at a slower rate than the 15-week-old mice injected with the full amount of Tam and died ~40 days after injection, likely due to less efficient excision of *Mecp2*. Importantly, however, these 15-week-old injected mice still developed symptoms and died at a significantly accelerated rate when compared with the 10-week-old injected mice (compare Supplementary Material, Fig. S1E and F to Fig. 1F and (15)). Finally, our data show that the accelerated RTT-like symptom onset and progression in 15 weeks of age or later was not specific to the RTT mouse model used or *Mecp2* mutation because we obtained similar results when a different floxed *Mecp2* mouse line (5) was used to generate Tam-inducible *Mecp2*$^{loxB/y}$*/CreER* mice, and excision was induced at 15 weeks of age. Specifically, these animals developed rapid and severe RTT-like symptoms reaching a score of 7–8 within 8 days followed by rapid lethality (Supplementary Material, Fig. S1G and H).

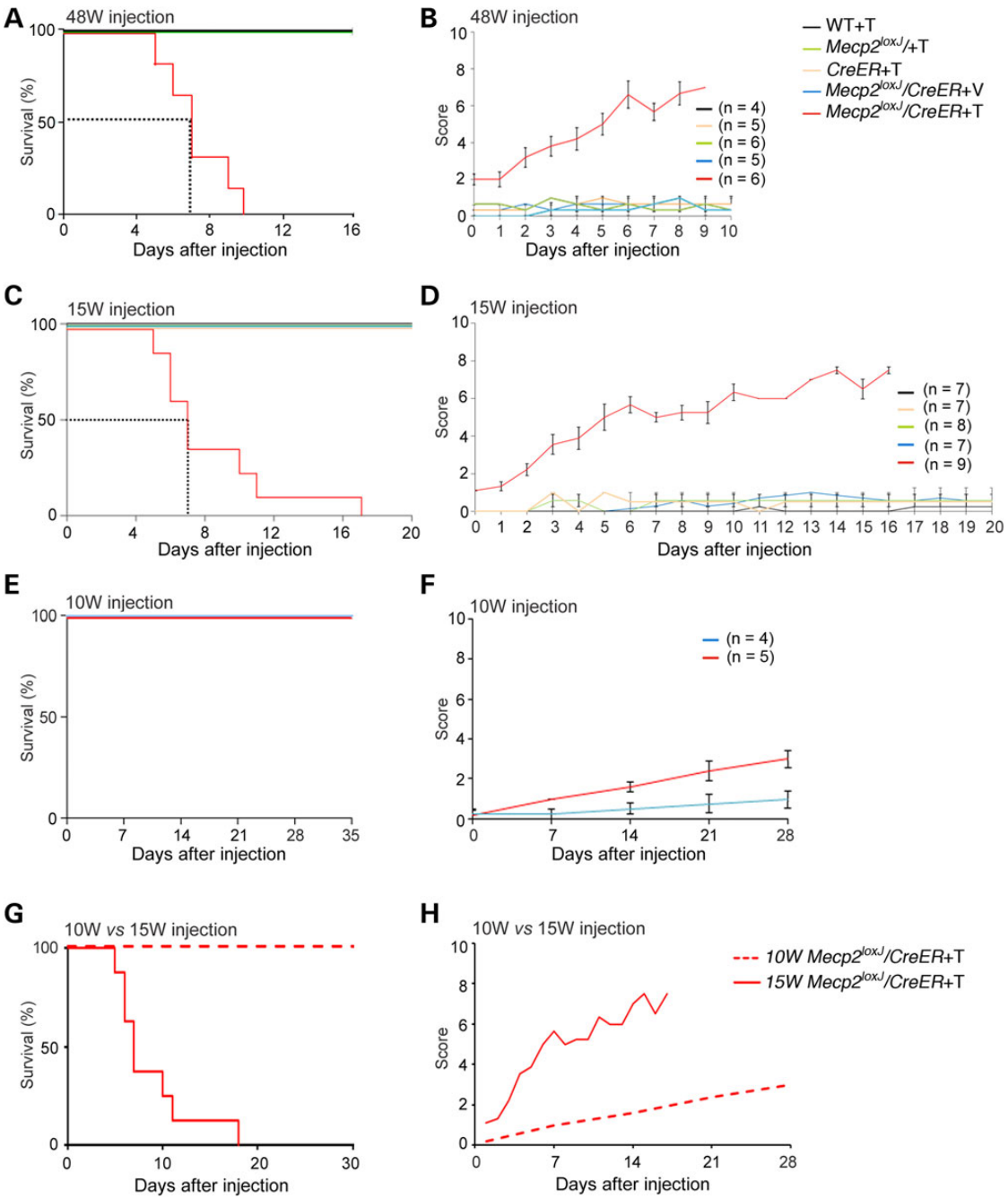

Figure 1. The depletion of MeCP2 at advanced adult stages induces rapid onset of RTT-like symptoms followed by death in few days. The Kaplan–Meier survival time course (**A** and **C**) and the phenotypic scores (**B** and **D**) of the 48 W- (A and B) and the 15 W- (C and D) Tam-injected *Mecp2*$^{loxJ/y}$/*CreER* male mice and the indicated control littermates (Veh-injected *Mecp2*$^{loxJ/y}$/*CreER*, and Tam-injected WT, *CreER* and *Mecp2*^{loxJ} male mice). Note that, one outlier 15 W-Tam-injected *Mecp2*$^{loxJ/y}$/*CreER* mouse that survived for 27 days was removed from the analysis because the analysis of MeCP2 revealed higher levels of residual MeCP2 than the average (~35% versus average of 20–25%). Error bars are mean ± SEM. The Kaplan–Meier survival time course (**E**) and the phenotypic scores (**F**) of the 10 W *Mecp2*^{loxJ}/*CreER* mice injected with Tam in parallel with 15 W *Mecp2*^{loxJ}/*CreER* mice (C and D) and the control age-matched littermate male mice (Veh-injected *Mecp2*^{loxJ}/*CreER*). (**G** and **H**) Overlay of survival curves and the aggregate symptom scores of the 15 W- and the 10 W-Tam *Mecp2*^{loxJ}/*CreER* mice. In all graphs, mice were injected with the standard 100 mg Tam per kg body weight for 7 consecutive days and the time points reflect time after the last of the 7 daily injections. Error bars are mean ± SEM.

Based on these collective data, we defined 15 weeks of age as a beginning of a transitional developmental stage at which MeCP2 becomes highly critical and remains highly critical thereafter for constitutive brain function and survival and where its loss results in immediate and severe RTT phenotype and lethality with almost no latency.

Depletion of MeCP2 at advanced adult stages induces rapid cellular changes including reduction in the size of neuronal nuclei and, ultimately, shrinkage of the brain

Because MeCP2 becomes highly critical during the transition between 10 and 15 weeks of age and remains critical thereafter, we focused our brain analyses mainly on mice of 15 weeks of age. We

first analyzed the levels of MeCP2 protein when the mice were highly symptomatic between 7 and 15 days post the last Tam injection. Quantitative western blot analysis showed reduction of MeCP2 protein to 20–25% of control levels in the whole brain, as well as in the hippocampus and the cortex of the 15 W-Tam-injected *Mecp2*$^{loxJ/y}$*/CreER* mice (Fig. 2A). Furthermore, immunohistochemical analysis confirmed that MeCP2 was undetectable in most neurons and astrocytes in the hippocampus (Fig. 2B and C) and cortex (Supplementary Material, Fig. S2) of 15 W-Tam-injected *Mecp2*$^{loxJ/y}$*/CreER* mice.

To further exclude the possibility that Tam injections in 15-week-old mice may result in accelerated rate of MeCP2 depletion compared with 10-week-old Tam-injected mice, thereby causing the appearance of sudden symptoms in the 15-week-old mice, we performed a time course analysis of the extent of *Mecp2* allele excision and reduction in the relative levels of MeCP2 protein from the first Tam injection. Our data show that although the excision of the *Mecp2* gene was rapid and completed by Day 7 from the first Tam injection, the depletion of MeCP2 protein occurred at a much slower rate (Supplementary Material, Fig. S3A and B).

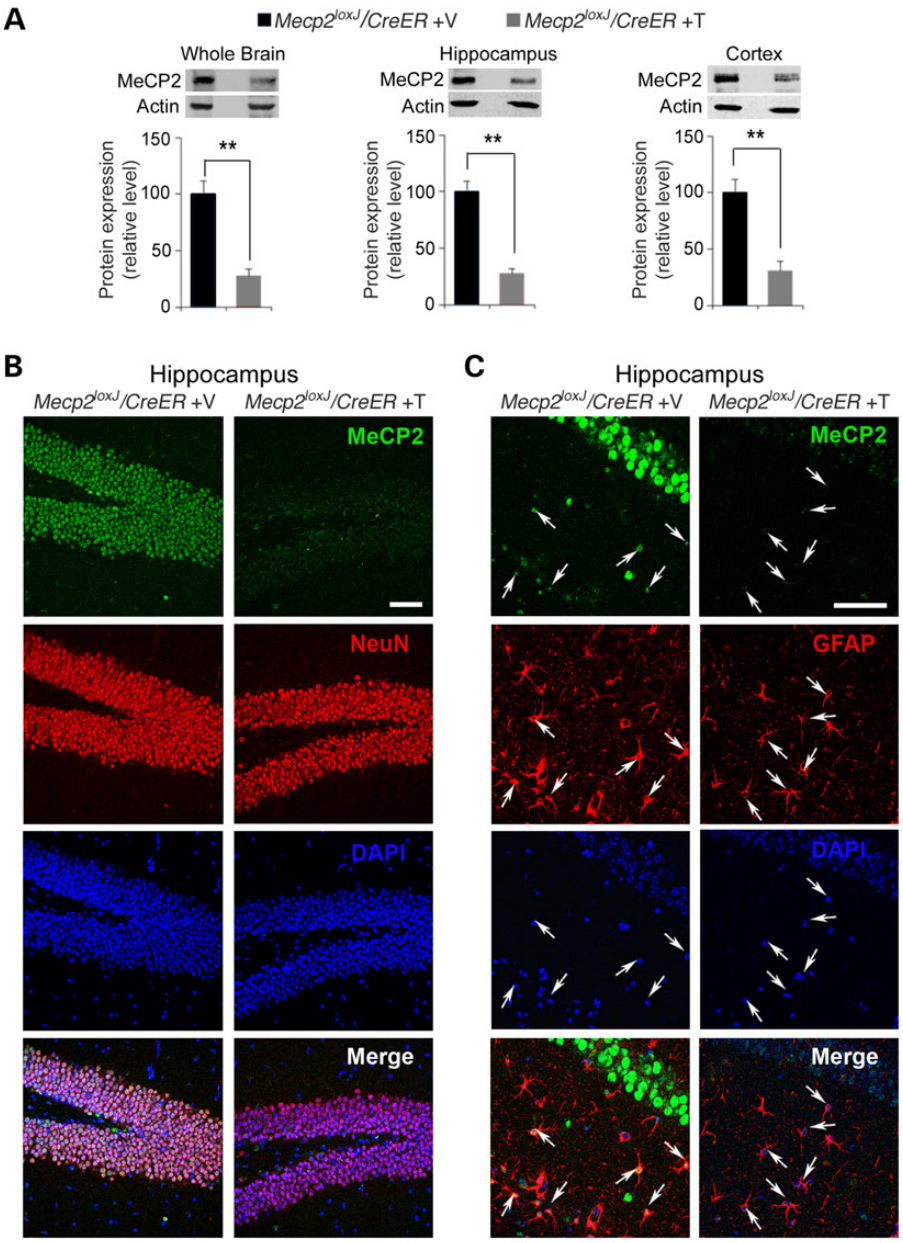

Figure 2. The efficient depletion of MeCP2 in the brains of *Mecp2*$^{loxJ/y}$*/CreER* mice injected with Tam at 15 weeks of age. (**A**) Quantitative western blot analysis showing the MeCP2 protein levels in the whole brain, hippocampus and cortex of 15 W-Tam- or Veh-injected *Mecp2*^{loxJ}*/CreER* male mice. The Mann–Whitney *U*-test was used to compare between Veh- and Tam-injected groups. Error bars are mean ± SEM. $^{**}P < 0.01$. $n = 3$ mice per group. (**B**) Representative images showing the hippocampus (dentate gyrus area) of 15 W-Tam- or Veh-injected *Mecp2*^{loxJ}*/CreER* male mice, immunolabeled for MeCP2 (green) and NeuN (red). DAPI (blue) represents nuclear staining. (**C**) Representative images of CA1 hippocampal area of 15 W-Tam- or Veh-injected *Mecp2*^{loxJ}*/CreER* mice immunolabeled for MeCP2 (green) and GFAP (red). Scale bars, 50 µm. All the brains were analyzed 1–2 week(s) post the last injection, when the Tam-injected mice developed severe symptoms and completely lost mobility. The Veh-injected control littermate's brains were collected at the same time as the Tam-injected ones.

Specifically, whereas at Days 5, 7 and 9 from the first Tam injection, the excision of the *Mecp2* allele reached 70, 83 and 84%, the MeCP2 protein level was reduced gradually by 20, 40 and 55%, respectively (Supplementary Material, Fig. S3A and B). In addition, we compared the MeCP2 protein levels of 5-, 10- and 15-week-old mice, immediately after the 7 days of Tam injection (Day 7) and showed that in all three age groups the MeCP2 protein was reduced similarly and by 40% (Supplementary Material, Fig. S3C). Importantly, we showed that in 10-week-old mice, even when MeCP2 protein was depleted already by 75% at 4 weeks after injection (28 days) and remained at this level at 8 weeks (56 days) after injection (Supplementary Material, Fig. S3D), these mice exhibited a score of 2 at 4 weeks after injection [Fig. 1H and (15)] and reached a score of 5 only after 8 weeks from Tam injection (15). In contrast, in 15-week-old mice, symptoms started to appear already when the level of the MeCP2 protein was reduced by ~60%, i.e. before it had reached the maximal level of 75% reduction (Fig. 1D and Supplementary Material, Fig. S3B), and progressed rapidly over the course of a few days (Fig. 1D). These data together, further show that the slow versus accelerated rate of symptom development at 10 and 15 weeks of age, respectively, is not due to differences in the rates of MeCP2 protein depletion, but rather likely due to changes occurring in the maturing brain between these two distinct stages.

Next, we analyzed the brain weights of the severely symptomatic Tam-injected *Mecp2*$^{loxJ/y}$*/CreER* mice (within a week from the last injection) and compared with that of the control age-matched littermates. We found that the removal of MeCP2 upon Tam treatment of 15-week-old *Mecp2*$^{loxJ/y}$*/CreER* mice resulted in significant reduction in the brain weight (to 93% of control values), when compared with control littermate mice (Fig. 3A). Similar results were obtained when MeCP2 was removed at 20, 34 or 48 weeks of age (Fig. 3B). These results are consistent with our previous studies showing a progressive shrinkage of the brain after MeCP2 removal at 5 or 10 weeks of age (15). However, while the reduction of the brain weight appeared immediately after MeCP2 removal at 15 weeks of age or later, it took several weeks for the brain to begin shrinking when MeCP2 was removed at earlier ages [5 or 10 weeks of age (15)]. This global anatomical abnormality of the brain correlated with changes at the cellular level. Specifically, there was a significant reduction in the nuclear size (reduced to 85% of controls) in neurons in the CA1 area of the hippocampus when compared with that of the Veh-injected *Mecp2*$^{loxJ/y}$*/CreER* age-matched littermates (Fig. 3C–E). Such reduction in the size of neuronal nuclei has been reported previously for mice with germline mutations in *Mecp2* (1) and neurons derived from ES cells lacking MeCP2 (7). These data suggest that similar events may occur when MeCP2 is removed at advanced adult stages, i.e. 15 weeks of age or later, however with extremely enhanced kinetics.

The loss of MeCP2 at advanced adult stages results in rapid aberration in dendritic arbor structures and the down-regulation of specific synaptic proteins

We next asked to what extent the acute loss of MeCP2 could affect the neuronal structural plasticity in such a short time, using hippocampal dendritic structures as proxy. This was accomplished using Golgi impregnation combined with neuronal 3D reconstruction. Intriguingly, within days post Tam injection, we found that the CA1 pyramidal neurons of the symptomatic 15 W-Tam-injected *Mecp2*$^{loxJ/y}$*/CreER* mice exhibited significantly fewer and shorter basal dendritic branches when compared with the 15 W-Veh-injected *Mecp2*$^{loxJ/y}$*/CreER* age-matched littermates (Fig. 4A, C and D). Furthermore, we found similar dramatic reduction in dendritic complexity, within days post Tam injection, when MeCP2 was removed at 20 (Fig. 4B,E and F), 34 or 48 weeks of age (Supplementary Material, Fig. S4A–F). These data are in line with the reduced dendritic complexity found at 5 and 10 W Tam-injected mice at their symptomatic stage (15). Our analysis further showed robust and similar reduction (to 50–60% of controls) in spine density of the basal dendrites of pyramidal neurons of all symptomatic *Mecp2*$^{loxJ/y}$*/CreER* mice, injected with Tam between 15 and 48 weeks of age, when compared with their Veh-injected *Mecp2*$^{loxJ/y}$*/CreER* age-matched littermates (Fig. 4G–J and Supplementary Material, Fig. S4G–J). Additionally, swelling aberrations in dendritic spines were also apparent (Fig. 4G, I and Supplementary Material, Fig. S4G and I). In contrast to 5 and 10 W Tam-injected mice, where both the basal and apical dendrites were affected, only the basal dendritic complexity was significantly affected in the symptomatic 15-, 20-, 34- and 48 W-Tam-injected *Mecp2*$^{loxJ/y}$*/CreER* mice when compared with those of the Veh-injected control age-matched littermates (Fig. 4, Supplementary Material, Figs S4 and S5).

Importantly, the rapid changes in the basal dendritic arbor structures when MeCP2 was removed at 15 weeks of age or later stands in contrast to the slow kinetics of dendritic changes when MeCP2 was removed at 10 weeks of age. Specifically, while removal of MeCP2 at 15 weeks of age or later resulted in >50% reduction in dendritic length and spine density within few days (Fig. 4 and Supplementary Material, Fig. S4), removal of MeCP2 at 10 weeks of age resulted in 25% reduction in dendritic length after 4 weeks when compared with control mice whose dendrites continue to increase in length, and in only 10% reduction when compared with the dendritic length of Tam-injected mice right after the last injection (Supplementary Material, Fig. S6). Furthermore, no change in spine density was observed even after 4 weeks when MeCP2 was removed at 10 weeks of age (Supplementary Material, Fig. S6). Only after 18 weeks more significant reduction was observed in dendritic length and reduction in spine density became apparent (Supplementary Material, Fig. S6) and even then it was less robust than in mice that lost MeCP2 at 15 weeks of age or at later time. The slow versus rapid kinetics of cellular changes mediated by the loss of MeCP2 at 10 and 15 weeks of age (or later), respectively, correlate with the slow versus rapid manifestation of severe RTT-like symptoms at these two ages.

Because 15 weeks of age represents the transition to the adult stage where removal of MeCP2 resulted in accelerated RTT-like disease progression, we sought to decipher the molecular changes that may underlie the morphological abnormalities observed at this stage. Our previous study, and those of others, indicated that some excitatory/inhibitory and pre-/post-synaptic proteins were dysregulated in mouse brain that lacks MeCP2 (12,15,21). We therefore analyzed the expression levels of several known synaptic proteins with key roles in the synaptic structure and plasticity identified in our previous study. Western blot analysis showed a significant reduction in the expression levels of several synaptic proteins in 15 W-Tam-injected *Mecp2*$^{loxJ/y}$*/CreER* mice compared with 15 W-Veh-injected *Mecp2*$^{loxJ/y}$*/CreER* littermates, including synapsin 1 (SYN1) (to 25%), VGLUT1 (to 40%), and NMDAR2A (to 40%) (Fig. 5). Immunostaining of the hippocampus for VGLUT1 and SYN1 confirmed their reduced expression levels (to ~40% of control) in symptomatic 15 W-Tam-injected *Mecp2*$^{loxJ/y}$*/CreER* mice (Supplementary Material, Fig. S7A–C). In contrast, we did not observe significant changes in CaMKIIα, CaMKIIβ, gamma-aminobutyric acid type B receptor subunit 2 (GABABR2), GluR2/3, PSD93 and Synaptotagmin 1 (SYT1) levels (Fig. 5). We further extended our analysis by

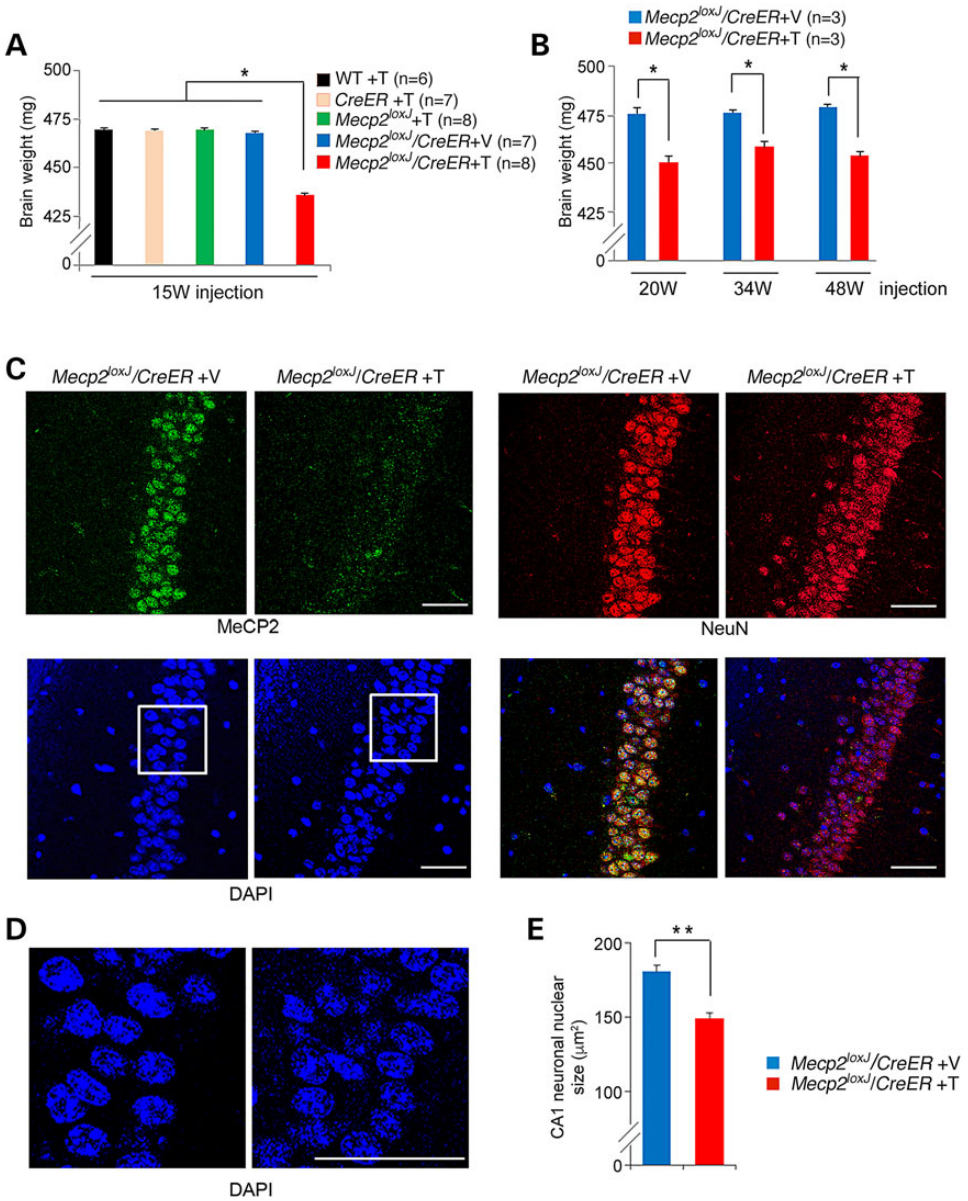

Figure 3. MeCP2 depletion at advanced adult stages leads to rapid shrinkage of the brain and reduction in nuclear size of hippocampal neurons. (**A**) The brains of the symptomatic 15 W-Tam-injected *Mecp2*^{loxJ}*/CreER* male mice are smaller than those of their age-matched control littermates. The brain weights were measured 5–15 days post-injection, when the Tam-injected *Mecp2*^{loxJ}*/CreER* mice were severely symptomatic. One-way ANOVA followed by appropriate *post hoc* for multiple-comparisons test was used to determine differences between groups. Error bars are mean ± SEM. *$P < 0.05$. (**B**) The brains of the symptomatic 20 W-, 34 W- and 48 W-Tam-injected *Mecp2*^{loxJ}*/CreER* mice become smaller than the brains of the control Veh-injected *Mecp2*^{loxJ}*/CreER* mice within days after Tam injection. The Mann–Whitney *U*-test was used to compare between Veh- and Tam-injected animals of each age group. Error bars are mean ± SEM. *$P < 0.05$. (**C**) Representative images of immunostaining of the CA1 area of the hippocampus of 15 W-Tam- or Veh-injected *Mecp2*^{loxJ}*/CreER* male mice at their symptomatic stage (score of 6–7, see Fig.1) immunolabeled for MeCP2 (green) and NeuN (red). DAPI (blue) represents nuclear staining. (**D**) Enlargement of the CA1 area (framed areas in C) showing smaller nuclei in CA1 hippocampal neurons of symptomatic 15 W-Tam-injected *Mecp2*^{loxJ}*/CreER* male mice compared to the Veh-injected littermate control male mice. (**E**) Nuclear size quantification data revealing smaller nuclei of the CA1 hippocampal neurons of the 15 W-Tam-injected *Mecp2*^{loxJ}*/CreER* mice at their symptomatic stage (score of 6–7) than those of the 15 W-Veh-injected *Mecp2*^{loxJ}*/CreER* control littermate mice. *t*-test was used to compare within Veh- and Tam-injected groups. Error bars are mean ± SEM. **$P < 0.01$. $n = 3$ mice per group. $n = 20$ neurons per animal. Scale bars, 50 µm.

evaluating the expression of the autism-related post-synaptic scaffolding protein family SHANK1, SHANK2 and SHANK3 involved in the organization of the post-synaptic density (22). Whereas SHANK1 and SHANK2 were significantly reduced (to ~50%) in symptomatic 15 W-Tam-injected *Mecp2*$^{loxJ/y}$*/CreER* mice, there was no effect on SHANK3 (Fig. 5). These results indicate specific rather than global regulation of the synaptic protein levels. To confirm that the altered protein levels caused by the depletion of MeCP2 also occurred at a later stage, we examined the synaptic protein expression levels in symptomatic 34 W-Tam-injected *Mecp2*$^{loxJ/y}$*/CreER* mice. The changes in protein levels were identical to those observed in 15 W-Tam-injected *Mecp2*$^{loxJ/y}$*/CreER* mice (Supplementary Material, Fig. S8) consistent with the morphological and survival results.

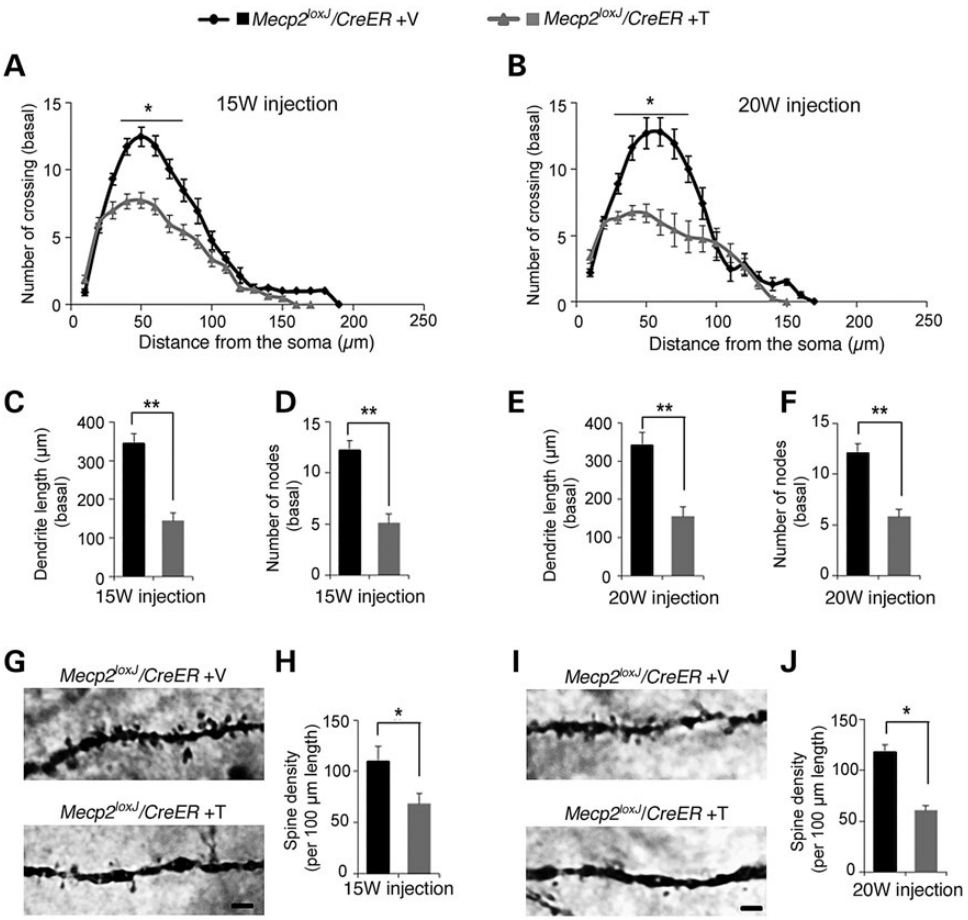

Figure 4. MeCP2 depletion at different advanced adult ages leads to rapid and severe reduction in the dendritic complexity of hippocampal pyramidal neurons. (**A** and **B**) Sholl analysis of CA1 pyramidal neurons of the symptomatic 15 W- (A) and 20 W- (B) Tam-injected *Mecp2*^{loxJ}*/CreER* mice shows that the basal dendrites of CA1 pyramidal neurons are significantly less complex than those of the Veh-injected *Mecp2*^{loxJ}*/CreER* age-matched littermate mice. Two-way repeated-measures ANOVA followed by appropriate *post hoc* for multiple-comparisons test was used to determine differences within Veh- and Tam-injected groups. Error bars are mean ± SEM. *$P < 0.05$. (**C–F**) Branch analyses of the CA1 pyramidal neurons of the symptomatic 15 W- (C and D) and 20 W- (E and F) Tam-injected *Mecp2*^{loxJ}*/CreER* male mice exhibit shorter basal dendritic branch length (C and E) and fewer numbers of nodes (D and F). *t*-test was used to compare between Veh- and Tam-injected animals of each age groups. Error bars are mean ± SEM. **$P < 0.01$. (**G–J**) CA1 pyramidal neurons of the symptomatic 15 W- (G and H) and 20 W- (I and J) Tam-injected *Mecp2*^{loxJ}*/CreER* male mice exhibit structural abnormalities in dendritic spines and reduced spine density. Representative images of dendrites of CA1 pyramidal neurons showing structural abnormalities in dendritic spines of symptomatic 15 W- (G) and 20 W- (I) Tam-injected *Mecp2*^{loxJ}*/CreER* male mice when compared with that of the Veh-injected mice. Scale bars, 2 μm. CA1 pyramidal neurons of 15 W- (H) and 20 W- (J) Tam-injected *Mecp2*^{loxJ}*/CreER* mice demonstrate significant reduction in dendritic spine density. Spine density per 100 μm length was measured on secondary dendrites. *t*-test was used to compare within Veh- and Tam-injected animals of each age groups. Error bars are mean ± SEM. *$P < 0.05$. $n = 4$ mice per genotype and age. $n = 12$ neurons per animal for all dendritic and spine analyses.

The dendritic complexity and the levels of specific synaptic proteins continue to increase in normal brain between early (adolescent) and later adult stages

To understand why there was a discrete transition in the consequences of MeCP2 depletion at 15 weeks of age, we examined several parameters of brain maturation in normal mice between 10 and 15 weeks of age. Interestingly, we found that the brain continues to increase in size until 15 weeks of age and then plateaus (Fig. 6A and B). Furthermore, the CA1 pyramidal neurons continue to gain dendritic complexity between 10 and 15 weeks of age (Fig. 6C), as indicated by their basal dendritic branches in 15-week-old mice, which are longer (Fig. 6D) and more branched with an increase number of nodes (Fig. 6E) than in 10-week-old mice. In contrast, the apical dendritic branches and the spine density remain unchanged between these two developmental stages (Fig. 6F–J). We also evaluated the synaptic protein levels. We found that while MeCP2 levels remain similar between 10 and 15 weeks of age, the levels of the specific synaptic proteins that were reduced upon MeCP2 elimination in the symptomatic 15- and 34 W-Tam-injected *Mecp2*$^{loxJ/y}$*/CreER* mice (SYN1, VGLUT1, NMDR2A, SHANK1 and SHANK2) increased over time between 5 and 15 weeks of age, and specifically between 10 and 15 weeks of age of normal mice (Fig. 7). In contrast, the levels of the proteins that were not affected by MeCP2 elimination (CaMKIIα, CaMKIIβ, GABABR2, Glut2/3, PSD93 and SHANK3) remained unchanged between 5, 10 and 15 weeks of age (Fig. 7). These data together indicate that the mouse brain continues to mature between 10 and 15 weeks of age and that the loss of MeCP2 at 15 weeks or later specifically affects parameters of neuronal maturation occurring during this transition.

Discussion

Germline mutations in the MECP2 gene manifest in onset of RTT phenotype in girls between 12 and 18 months of age and in male

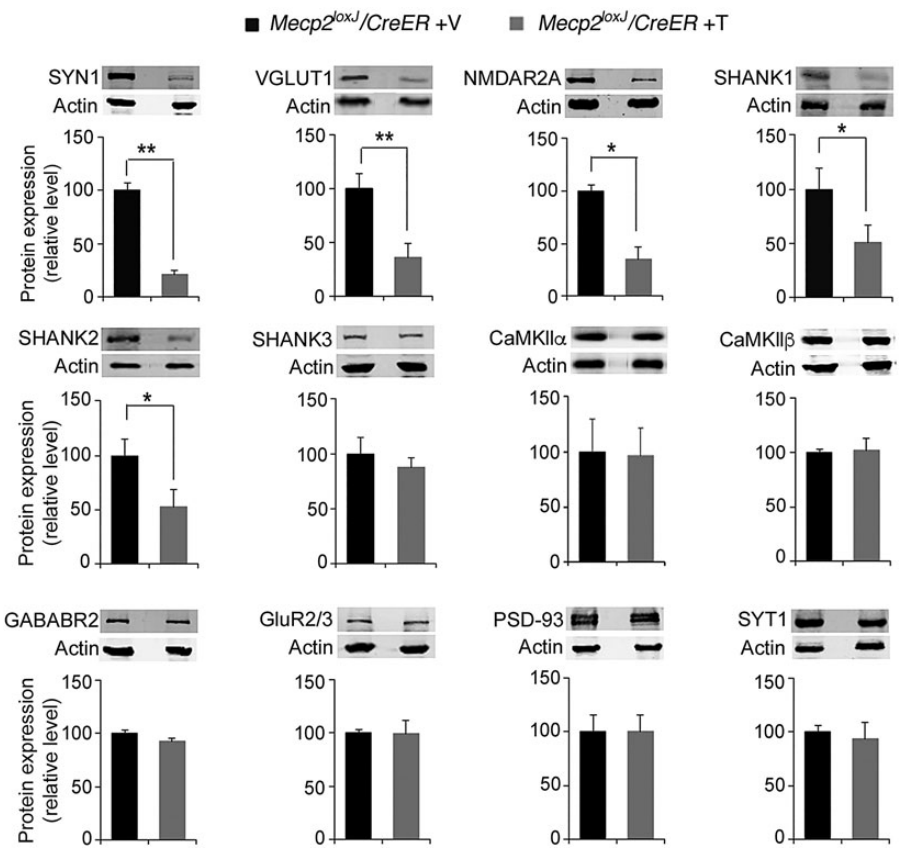

Figure 5. Specific reduction in synaptic protein levels upon MeCP2 depletion at an advanced adult stage. Quantitative western blot analysis showing significant reduction in the levels of selective synaptic proteins in the whole brains of 15 W-Tam-injected *Mecp2*^{loxJ}*/CreER* male mice when compared with the brains of the 15 W-Veh-injected *Mecp2*^{loxJ}*/CreER* littermate control male mice. The Mann–Whitney *U*-test was used to compare within Veh- and Tam-injected groups. Error bars are mean ± SEM. $^{*}P < 0.05$, $^{**}P < 0.01$. $n = 3$ mice per group.

mouse models between 4 and 5 weeks of age (juvenile) (4). In the normal mouse brain, neuronal MeCP2 is expressed to higher levels at this postnatal developmental stage than at birth (6). Together, these results led initially to the notion that MeCP2 is critical for synaptogenesis and brain maturation during this postnatal developmental stage. However, more recent studies including our own, indicate that the predominant function of MeCP2 is more likely to maintain the proper structure/function of the mature neuronal networks (Fig. 8). Specifically (i) RTT-like symptoms can be reversed in mice by reactivation of MeCP2 even at late adolescent/adult stages when the mice are symptomatic (23–25), (ii) removal of MeCP2 even at the early adult stage can cause severe RTT-like phenotypes including lethality in male mice (15–17) and severe RTT-like phenotypes in female mice (15), indistinguishable from classic RTT phenotypes caused by germline mutations in MeCP2 (1,5) and (iii) the brain anatomy and neuronal structure abnormalities acquired by inducible loss of MeCP2 at juvenile or early adult stages (15) are typical for classic RTT (1,6). Thus, these findings support the idea that although developmental in onset, MeCP2 is required for maintaining mature neuronal networks throughout life.

Here, we revealed a previously unrecognized highly critical developmental stage, which requires immediate MeCP2 function for continuous functioning and stabilization of the mature neuronal networks. This stage coincides with the transition from adolescent to adult stage, a time at which the brain reaches full maturation. Most strikingly, the loss of MeCP2 at this transitional stage (15 weeks of age), and thereafter, resulted in rapid development of severe RTT-like symptoms and incompatibility with life within only few days (Fig. 8). Such acute requirement for MeCP2 presence contrasts with the latency in classic RTT or even the much slower kinetics of symptom appearance and progression if MeCP2 is lost at the earlier juvenile and adolescent stages (15). In a previous study by Cheval *et al.* (16), removal of MeCP2 by Tam, at 3, 11 or even 20 weeks of age, all resulted in a median survival time of 39 weeks (35, 27 and 18 weeks post Tam injection, respectively). These results stand in contrast to our study herein showing that the median survival time of mice injected with Tam at 20 weeks of age is 4 days. They also stand in contrast to our previous studies (15) and studies by McGraw *et al.* (17) showing that excision of MeCP2 at 5, 8 or 10 weeks of age all resulted in median survival times between 13 and 16 weeks from Tam injection (depending on the mouse model used). The difference between our results and those of Cheval *et al.* is not due to different mouse models because we confirmed our data with the same mouse model used in Cheval *et al.* (16) (Supplementary Material, Fig.S1G and H). Rather, it is likely due to differences in Tam efficacy reflecting differences in Tam preparation (active Tam in solution) and injection protocols. In support of this possibility, we showed that the rate of MeCP2 protein reduction in our study is different than Cheval *et al.* Specifically, while the MeCP2 protein level was gradually reduced by ~55% at Day 9 and by 70–75% between Days 20 and 24 from the first Tam injection (Fig. 2A and Supplementary Material, Fig. S3B), in Cheval *et al.* MeCP2 level was reduced by 20–25% at Day 5 and remained at the same level at Days 8 and 12, and was

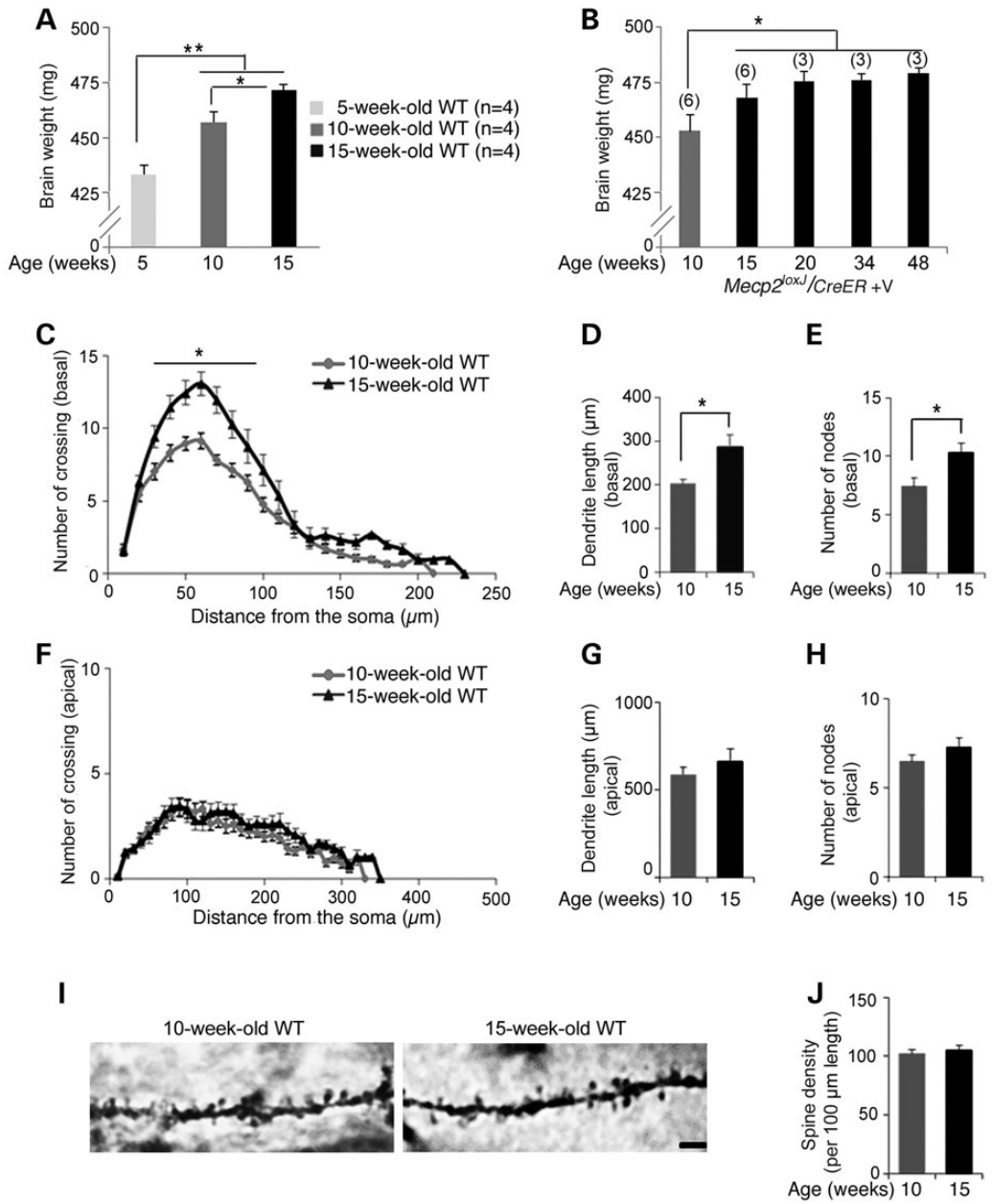

Figure 6. The normal mouse brain continues to mature between early adult and advanced adult stages. (**A** and **B**) Comparison of brain weight between the late juvenile stage (5 weeks of age), early adult (adolescent) stage (10 weeks of age) and adult stage (15 weeks of age and older) showing that the brain continues to increase in size even between 10 and 15 weeks of age after which it reaches saturation. One-way measures ANOVA followed by appropriate *post hoc* for multiple-comparisons test was used to determine differences in brain sizes. Error bars are mean ± SEM. $^{*}P < 0.05$ and $^{**}P < 0.01$. (**C–H**) Dendritic Scholl and branch analyses of hippocampal pyramidal neurons at 10 and 15 weeks of age. Sholl analysis (C and F) shows that the basal dendrites of CA1 pyramidal neurons (C) of the 15-week-old wild-type mice are significantly more complex than those of the 10-week-old wild-type mice while the apical dendrites (F) remain unchanged. Two-way repeated-measures ANOVA followed by appropriate *post hoc* for multiple-comparisons test was used to determine differences within 10- and 15-week-old mouse groups. Error bars are mean ± SEM. $^{*}P < 0.05$. CA1 pyramidal neurons of the 15-week-old wild-type mice exhibit longer basal dendritic branch length (D) and increased number of nodes (E), while in apical dendrites the parameters remain unchanged between 10 and 15 weeks of age (G–H). *t*-test was used to compare within 10- and 15-week-old mice groups. Error bars are mean ± SEM. $^{*}P < 0.05$. (**I**) Representative images of Camera lucida tracing of CA1 pyramidal neurons in the hippocampus showing structural similarities in spines on the associated secondary dendrites in 10- and 15-week-old wild-type mice. Scale bars, 2 μm. (**J**) CA1 pyramidal neurons of 10- and 15-week-old wild-type mice demonstrate similar dendritic spine densities. Spine density per 100 μm length was measured on secondary dendrites. *t*-test was used to determine differences in spine density. Error bars are mean ± SEM. $n = 3$ mice per genotype and age. $n = 12$ neurons per animal.

reduced by 70–75% only between 4 and 7 weeks from the first Tam injection. Such higher levels of residual MeCP2 likely extend the latency period even at the adult stage (15 weeks of age or later), which we showed requires the acute presence of MeCP2 for stabilization of the fully mature neuronal networks. It is also possible that the discrepancy between our study and that of Cheval *et al*. originated from disparities in the extent of MeCP2 protein reduction in the different brain areas. Our previous and present studies also analyzed the levels of the MeCP2 protein in different brain areas and showed similar extent of reduction [Fig. 2 and (15)], however, Cheval *et al*. analyzed only the whole brains and thus preventing direct comparisons. Importantly, we showed

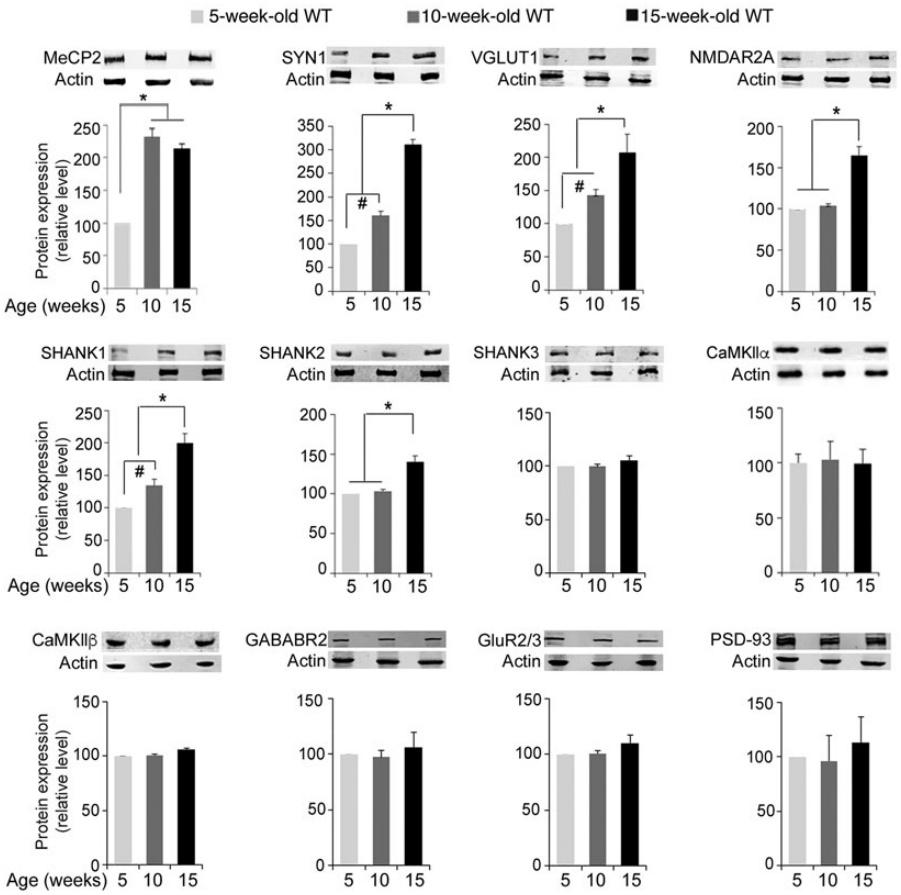

Figure 7. Progressive increases in the levels of specific synaptic proteins in the brain of normal mice between 5 and 15 weeks of age. Quantitative western blot analysis showing significant increases in the level of MeCP2 between 5 and 10 weeks of age, but not between 10 and 15 weeks of age, while the levels of specific synaptic proteins including SYN1, VGLUT1, NMDAR2A, SHANK1 and SHANK2 continue to increase in the brain of 15-week-old wild-type mice when compared with that of 10-week-old wild-type mice. Note that, the levels of other synaptic proteins such as CaMKIIα, CaMKIIβ, GABABR2, GluR2/3, PSD93 and SHANK3 do not change over this period of time. One-way measure ANOVA followed by appropriate *post hoc* for multiple-comparisons test was used to determine differences. Error bars are mean ± SEM. $^{*}P < 0.05$ and $^{\#}P < 0.05$. $n = 3$ mice per group.

that there is no difference in the rate of MeCP2 protein reduction after Tam injection between 5 and 10- and 15-week-old mice yet there are remarkable differences in the latency of symptom appearance, progression and lethality between juvenile (5-week-old)/adolescent (10-week-old) mice and adult mice (15 weeks old or older). In fact symptoms onset (score of 2) occurred in the Tam-injected 15-week-old mice even before the level of MeCP2 was reduced to its lowest level (~60% reduction) as opposed to much longer latency of symptom appearance in the Tam-injected 10-week-old mice even when MeCP2 was reduced already by 75–80%, lending further support to the idea that the MeCP2 level becomes highly critical for the proper function of this protein at the adult stage.

Nonetheless, as Cheval *et al.* suggested, the milder phenotypes and the longer survival of the mice in their study allowed them to unmask yet another critical time period, at 39 weeks of age, which likely reflects the aging process and the important presence of normal MeCP2 levels in this period (16). It is possible that the effect of MeCP2 depletion specifically at 48 weeks of age in our study is also associated with aging. In support of this view, the dendritic complexity, specifically dendritic length, of the control mice was reduced at 48 weeks of age when compared with 15, 20 or 34 weeks of age (Supplementary Material, Fig. S4B versus Fig. 4A and B and Supplementary Material, Fig. S4A).

Our finding showing that the loss of MeCP2 in mice as early as 15 weeks of age and beyond results in a robust and rapid manifestation of RTT phenotypes, followed by lethality within days, is clearly not reflective of an aging process, but rather reflects a period of highly critical and dynamic function of MeCP2 during the final stages of neuronal network maturation (Fig. 8). In support of this model, we found that in normal mice between 10 and 15 weeks of age, there is a significant increase in the brain size and in neuronal dendritic complexity, specifically in basal dendrites. Additionally, levels of several synaptic proteins were also up-regulated during this same time period. Interestingly, within a few days of removal of MeCP2 at 15 weeks of age or later, there occurred a significant and specific reduction in the complexity of the basal, but not the apical dendrites. There was also down-regulation specifically of the synaptic proteins, whose levels increased in the normal brain during this period. Thus, it is likely, that maintenance of this final stage of neuronal network maturation requires the persistent function of MeCP2. Interestingly, the levels of MeCP2 protein remain unchanged during this transitional period to adult stage, indicating that it is the function and not the level of MeCP2 that becomes highly critical. It is well known that certain phenomena, such as synaptic strengthening, are regulated by different mechanisms, such as through phosphorylation, at different postnatal stages, including

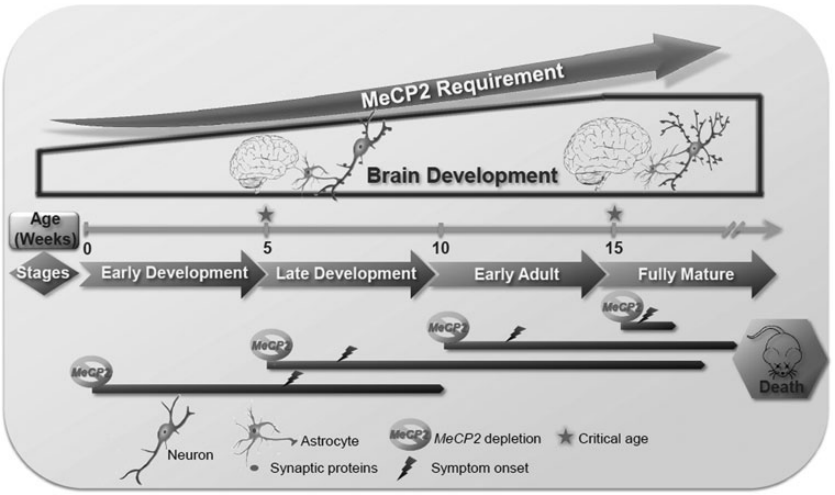

Figure 8. Schematic model describing the essential function of MeCP2 during postnatal developmental stages. During normal postnatal development, neurons as well as and astrocytes mature, evident by increasing dendritic complexity and synaptogenesis concomitant with increased expression of specific synaptic proteins. Our studies and those of others (1,5,6,15–17) indicate that germline (classic RTT) and conditional postnatal loss of MeCP2 at late juvenile (5 weeks), early adult (10) or even advanced adult stages (15 weeks or later), all result in severe RTT-like phenotypes and premature lethality in male mice, and the brain acquires similar anatomical and cellular abnormalities. However, while the loss of MeCP2 at germline, 5 and 10 W stages result in symptoms with a latency of weeks, the loss of MeCP2 at more advanced adult stages (15 W or later) reduces latency to only a few days, along with a reduction of brain weight, regression of dendritic arborization and astrocyte process complexity, and reduced levels of essential synaptic proteins. Thus, we propose two critical time points for the MeCP2 function during postnatal development of the brain: (i) 5 weeks of age, corresponding to the symptom onset in the classic RTT due to germline mutations, or by induced loss of MeCP2 between 5 and 10 weeks of age, corresponding to gradual (within weeks) symptom onset, and (ii) 15 weeks of age or later when the absence of MeCP2 affects immediately and severely the mature brain structure and function leading to severe RTT symptoms premature lethality within few days.

mature adult stage (19), thus it is likely that MeCP2 functions differentially, at different postnatal stages. There is also increasing evidence for large-scale homeostatic structural changes, such as dendritic arbor dynamics, associated with functional compensation of the fully developed neural networks in the adult brain (19,26). It is possible that MeCP2 has critical function in such dynamic structural changes, which are highly important for the stability of the neural networks. How might MeCP2 regulate the levels of the specific synaptic proteins? In our previous study, we showed that although there was a significant reduction in the level of specific synaptic proteins when the MeCP2 loss was induced postnatally, the levels of their mRNA remained unchanged (15). Thus, MeCP2 most likely regulates the levels of these synaptic proteins post-transcriptionally, directly or indirectly. In the normal brain, dendritic arbor growth is highly dynamic and synaptic strength and branch stability are concurrent, thus the reduction in synaptic proteins upon the loss of MeCP2 most likely mediates the reduction in the complexity of dendritic arbor structures. However, it is also possible that the loss of dendritic arbors and synaptic contacts induces degradation of proteins localized within these compartments, in which case, the reduction in synaptic protein levels may represent the secondary effect of the loss of MeCP2.

Our previous studies and those of others showed that glia, and specifically astrocytes, contribute significantly to RTT neuropathology (25,27–30). In addition, our previous study showed that removal of MeCP2 at 5 or 10 weeks of age results not only in retraction of dendritic arbor structures of neurons, but also in retraction of astrocytic processes (15) (Fig. 8). Interestingly, we found that in normal mice not only dendritic arbor structures but also astrocytic processes continue to mature, reaching higher levels of complexity between 10 and 15 weeks of age, and that removal of MeCP2 at 15 weeks of age or later results in retraction of both, neuronal processes as well as astrocytic processes within days (Fig. 4 and data not shown). Because astrocytes not only provide metabolic support to neurons, but also function as an integral part of synapses, with their processes ensheathing synapses (31), such rapid alteration in complexity of both astrocytic and neuronal processes might be expected to collapse neuronal circuitry throughout the brain.

In sum, our findings provide further insight into the function of MeCP2 at the different stages of brain maturation and support a highly critical role for MeCP2 as the neuronal networks reach its highest levels of maturation. Decreased levels of MeCP2 that impair its central function in the maintenance of the mature brain may also affect other types of neuropathology indirectly.

Materials and Methods

Animals

All animal studies were approved by the Institutional Animal Care and Use Committees at Stony Brook University and complied with the guidelines established by the National Institute of Health.

CreER [B6.Cg-Tg(CAG-cre/Esr1)5Amc/J] and *Mecp2*$^{loxB/y}$ (5) (B6;129P2-Mecp2tm1Bird/J) transgenic mice were obtained from the Jackson Laboratory. *CreER* [B6.Cg-Tg(CAG-cre/Esr1)5Amc/J] were maintained in a pure C57BL/6 background. The *Mecp2*$^{loxB/y}$ mice were backcrossed to C57BL/6 for eight generations. The *Mecp2*$^{loxJ/y}$ (1) (B6;129S4-*Mecp2*^{tm1Jae}/Mmcd) transgenic mice were obtained from MMRRC. To generate the double transgenic *Mecp2*$^{loxJ/y}$/*CreER* males, and all their control littermates (WT, *CreER* and *Mecp2*$^{loxJ/y}$ or *Mecp2*$^{loxJ/+}$), we crossed female mice heterozygous for the *Mecp2lox* allele (*Mecp2*$^{loxJ/+}$) with male mice heterozygous for the *CreER* transgene. Similar strategy was used to generate the *Mecp2*$^{loxB/y}$/*CreER* males and all the necessary control male mice. The flox and Cre sequences were identified by polymerase chain reaction (PCR) on tail biopsies with the following sets of primers: for *Mecp2*^{loxJ} allele, forward 5′-CAC CAC AGA AGT ACT ATG ATC-3′ and reverse 5′-CTA GGT AAG AGC TCT

TGT TGA-3′; for *Mecp2*^{loxB} allele, forward 5′-TGG TAA AGA CCC ATG TGA CCC AAG-3′ and reverse 5′-GGC TTG CCA CAT GAC AAG AC-3′; for the *CreER* allele, forward 5′-CCG TAC ACC AAA ATT TGC C-3′ and reverse 5′-ATC GCG AAC ATC TTC AGG-3′.

Tam treatment

Tam (Sigma) was prepared in the vehicle (Veh) solution consisting of 10% ethanol/90% sunflower oil (Sigma) as follows: 200 mg of Tam were suspended in 2 ml of ethanol in 50 ml Falcon tube and mixed thoroughly using a vortex at maximum speed for 10 min, then 18 ml of sunflower oil was added. The solution was sonicated three times for 5 min each on ice with a cooling period of 5 min on ice in between. Similar protocol (vortex and sonication) was performed in parallel without the Tam to prepare the Veh solution. Aliquots of 1 ml Tam or Veh solution were stored at −20°C and thawed before usage at 37°C for 15 min. *Mecp2*^{lox}*/CreER* male mice and their control age-matched littermates were treated by intra-peritoneal injection, at the indicated ages, with 100 mg/kg body weight of Tam or Veh, daily for 7 consecutive days. For some experiments indicated in the main text half the amount of Tam was injected daily for 14 consecutive days.

Phenotypic scoring

Male mice were scored daily (15 weeks of age or older) or weekly (10 weeks of age). Mice were removed from their home cage and placed onto a bench, at the same time during the day when possible. The scoring was performed essentially as we previously described (15). Each of the 5 symptoms, including mobility, gait, hindlimb clasping, tremor and general condition was scored as 0 (symptom absent), 1 (symptom present) or 2 (symptom severe).

DNA extraction and quantitative real-time PCR analysis

DNA was extracted from half-brains using the TRIzol extraction protocol (Life Technologies). The level of excision of the *Mecp2* allele was determined by quantitative real-time PCR using specific primers to amplify region within the floxed exon 3 of the *Mecp2* allele. The relative abundance was normalized to β-actin. Quantitative real-time PCR was performed in an ABI StepOnePlus real-time PCR system using SYBR-green PCR master mix (Applied Biosystems). The primers used were as follows: *Mecp2*, forward 5′-AGG CAG GCA AAG CAG AAA CAT CAG-3′ and reverse 5′-TCA TACTTT CCA GCA GAT CGG CCA-3′; β-actin, forward 5′-GGC TGT ATTCCC CTC CAT CG-3′ and reverse 5′-CCA GTT GGT AAC AAT GCCATG T-3′.

Western blot analysis

Whole-brain protein extracts were prepared from half-brain or the indicated brain areas using the Dignam method with some modifications (15). For synaptic proteins, half-brain tissues were homogenized in a Dounce homogenizer, in lysis buffer containing 5 mM sodium phosphate, pH 7.2, 320 mM sucrose, 1 mM sodium fluoride and 1 mM sodium orthovanadate and protease inhibitors (Roche), followed by passing through the 1 ml syringes with the 27-G needles for ten times. The lysates were centrifuged at 4°C for 15 min at 1250 × g. Supernatants were collected and western blotting was performed as described previously (15,27). The primary antibodies used were as follows: mouse anti-MeCP2 (Sigma, 1:5000), mouse anti-CaMKIIα (Calmodulin-Dependent Protein Kinase II α, Millipore, 1:2000), rabbit anti-CaMKIIβ (Calmodulin-Dependent Protein Kinase II β, Abcam, 1:10 000), rabbit anti-GluR2/3 (Glutamate Receptor 2/3, Millipore, 1:1000), mouse anti-GABABR2 (Neuromab, 1:2000), mouse anti-VGLUT1 (vesicular glutamate transporter 1, Neuromab, 1:500), rabbit anti-NMDAR2A (*N*-methyl-D-aspartate 2A, Abcam, 1:1000), rabbit anti-SYT1 (Synaptic Systems, 1:2000), rabbit anti-SYN1 (Abcam, 1:2500), mouse anti-PSD-93 (post-synaptic density protein 93, Neuromab, 1:5000), mouse anti-SHANK1 (Neuromab, 1:200), anti-SHANK2 (Neuromab, 1:100), anti-SHANK3 (Neuromab, 1:200) and rabbit anti-β-actin (Abcam, 1:5000) was used as loading control. The secondary antibodies used were IRDye800 or IRDye700-conjugated (LI-COR Biosciences) (1:10 000). Membranes were scanned using the Odyssey-Infrared Imaging System (LI-COR Biosciences), and the intensities of the bands of interest were determined from the captured images using the Odyssey imaging software.

Immunohistochemistry

Mice were fixed by transcardial perfusion with 4% paraformaldehyde in phosphate-buffered saline (PBS) as described (27). The brains were removed and post-fixed overnight with 4% paraformaldehyde at 4°C. The fixed tissue was cyroprotected with 30% sucrose in PBS buffer and frozen in the optimal cutting medium (Neg50, Richard-Allan Scientific). Coronal sections were obtained by sectioning the tissue on a HM505E Microm Cryostat (Cryostat Industries, Inc.) at 40 μm and preserved at −20°C in PBS-buffered 50% glycerol until analyzed. The sections were immunostained using chicken anti-MeCP2 antibody (a generous gift from J.M. LaSalle, University of California, Davis, CA, 1:10 000), rabbit anti-GFAP (Millipore Bioscience Research Reagents, 1:2000), mouse anti-NeuN (Millipore Bioscience Research Reagents, 1:200), rabbit anti-SYN1 (Abcam, 1:1000) and mouse anti-Vglut1 (Neuromab, 1:200) followed by incubation with the appropriate secondary antibodies conjugated to cyanine (Jackson ImmunoResearch). MeCP2 immunostaining was enhanced using biotinstreptavidin-conjugated secondary antibodies. Nuclei were counterstained with 4',6-diamidino-2-phenylindole (DAPI, Invitrogen). Images were collected on a Zeiss confocal laser scanning LSM 510 microscope. Mean area staining intensity for SYN1 and VGLUT1 was determined by using the ImageJ software (http://rsb.info.nih.gov/ij). The evaluation of nuclear size of neurons in the hippocampal CA1 area was performed by measuring the size of DAPI positive area, co-localized with NeuN labeling, by the ImageJ software.

Golgi staining

Golgi staining was carried out using a modified Golgi method (EZ Golgi method, Cornell University) and performed according to the manufacturer's instructions. The brains of Veh- or Tam-injected *MeCP2*$^{loxJ/y}$*/CreER* mice were incubated in the impregnation solution and sectioned at a thickness of 150 μm. The pyramidal neurons in the CA1 region of the hippocampus were traced and reconstructed using a camera lucida device blinded to genotype and treatment. Reconstructed neurons were analyzed using Neurolucida explorer software for spine density, branches and Sholl analysis as described previously (15).

Brain-weight assessment

Mice were anesthetized at the appropriate age with isoflurane and euthanized. The brains were harvested and immediately weighted. The whole brains were excised by a single cut at the caudal edge of the cerebellum between the brain and the spinal cord.

Statistical analysis

Data were analyzed using Student's *t*-test, the Mann–Whitney *U* test or analysis of variance (ANOVA-one-way, -two-way or

repeated-measures ANOVA as appropriate), with *post hoc* for multiple-comparisons test when required (Statview 5.0, SAS Institute, Inc.).

Supplementary Material

Supplementary Material is available at *HMG* online.

Acknowledgements

We thank Dr LaSalle for the anti-MeCP2 antibody, Dana Laikhram, Jenna Brunette and Shaun Charkowick for technical assistance.

Conflict of Interest statement. None declared.

Funding

The work was supported by the National Institute of Health (R01HD056503 to N.B. and G.M.). G.M. is an Investigator of the Howard Hughes Medical Institute.

References

1. Chen, R.Z., Akbarian, S., Tudor, M. and Jaenisch, R. (2001) Deficiency of methyl-CpG binding protein-2 in CNS neurons results in a Rett-like phenotype in mice. *Nat. Genet.*, **27**, 327–331.
2. Amir, R.E., Van den Veyver, I.B., Wan, M., Tran, C.Q., Francke, U. and Zoghbi, H.Y. (1999) Rett syndrome is caused by mutations in X-linked MECP2, encoding methyl-CpG-binding protein 2. *Nat. Genet.*, **23**, 185–188.
3. Armstrong, D.D. (2001) Rett syndrome neuropathology review 2000. *Brain Dev.*, **23**(Suppl. 1), S72–S76.
4. Chahrour, M. and Zoghbi, H.Y. (2007) The story of Rett syndrome: from clinic to neurobiology. *Neuron*, **56**, 422–437.
5. Guy, J., Hendrich, B., Holmes, M., Martin, J.E. and Bird, A. (2001) A mouse Mecp2-null mutation causes neurological symptoms that mimic Rett syndrome. *Nat. Genet.*, **27**, 322–326.
6. Kishi, N. and Macklis, J.D. (2004) MECP2 is progressively expressed in post-migratory neurons and is involved in neuronal maturation rather than cell fate decisions. *Mol. Cell. Neurosci.*, **27**, 306–321.
7. Yazdani, M., Deogracias, R., Guy, J., Poot, R.A., Bird, A. and Barde, Y.A. (2012) Disease modeling using embryonic stem cells: MeCP2 regulates nuclear size and RNA synthesis in neurons. *Stem Cells*, **30**, 2128–2139.
8. Belichenko, P.V., Oldfors, A., Hagberg, B. and Dahlstrom, A. (1994) Rett syndrome: 3-D confocal microscopy of cortical pyramidal dendrites and afferents. *Neuroreport*, **5**, 1509–1513.
9. Chapleau, C.A., Calfa, G.D., Lane, M.C., Albertson, A.J., Larimore, J.L., Kudo, S., Armstrong, D.L., Percy, A.K. and Pozzo-Miller, L. (2009) Dendritic spine pathologies in hippocampal pyramidal neurons from Rett syndrome brain and after expression of Rett-associated MECP2 mutations. *Neurobiol. Dis.*, **35**, 219–233.
10. Moretti, P., Levenson, J.M., Battaglia, F., Atkinson, R., Teague, R., Antalffy, B., Armstrong, D., Arancio, O., Sweatt, J.D. and Zoghbi, H.Y. (2006) Learning and memory and synaptic plasticity are impaired in a mouse model of Rett syndrome. *J. Neurosci.*, **26**, 319–327.
11. Asaka, Y., Jugloff, D.G., Zhang, L., Eubanks, J.H. and Fitzsimonds, R.M. (2006) Hippocampal synaptic plasticity is impaired in the Mecp2-null mouse model of Rett syndrome. *Neurobiol. Dis.*, **21**, 217–227.
12. Chao, H.T., Zoghbi, H.Y. and Rosenmund, C. (2007) MeCP2 controls excitatory synaptic strength by regulating glutamatergic synapse number. *Neuron*, **56**, 58–65.
13. Calfa, G., Li, W., Rutherford, J.M. and Pozzo-Miller, L. (2015) Excitation/inhibition imbalance and impaired synaptic inhibition in hippocampal area CA3 of Mecp2 knockout mice. *Hippocampus*, **25**, 159–168.
14. Zhang, W., Peterson, M., Beyer, B., Frankel, W.N. and Zhang, Z. W. (2014) Loss of MeCP2 from forebrain excitatory neurons leads to cortical hyperexcitation and seizures. *J. Neurosci.*, **34**, 2754–2763.
15. Nguyen, M.V., Du, F., Felice, C.A., Shan, X., Nigam, A., Mandel, G., Robinson, J.K. and Ballas, N. (2012) MeCP2 is critical for maintaining mature neuronal networks and global brain anatomy during late stages of postnatal brain development and in the mature adult brain. *J. Neurosci.*, **32**, 10021–10034.
16. Cheval, H., Guy, J., Merusi, C., De Sousa, D., Selfridge, J. and Bird, A. (2012) Postnatal inactivation reveals enhanced requirement for MeCP2 at distinct age windows. *Hum. Mol. Genet.*, **21**, 3806–3814.
17. McGraw, C.M., Samaco, R.C. and Zoghbi, H.Y. (2011) Adult neural function requires MeCP2. *Science*, **333**, 186.
18. Silva-Santos, S., van Woerden, G.M., Bruinsma, C.F., Mientjes, E., Jolfaei, M.A., Distel, B., Kushner, S.A. and Elgersma, Y. (2015) Ube3a reinstatement identifies distinct developmental windows in a murine Angelman syndrome model. *J. Clin. Invest.*, **125**, 2069–2076.
19. McCutcheon, J.E. and Marinelli, M. (2009) Age matters. *Eur. J. Neurosci.*, **29**, 997–1014.
20. Lebel, C. and Beaulieu, C. (2011) Longitudinal development of human brain wiring continues from childhood into adulthood. *J. Neurosci.*, **31**, 10937–10947.
21. Chao, H.T., Chen, H., Samaco, R.C., Xue, M., Chahrour, M., Yoo, J., Neul, J.L., Gong, S., Lu, H.C., Heintz, N. *et al.* (2010) Dysfunction in GABA signalling mediates autism-like stereotypies and Rett syndrome phenotypes. *Nature*, **468**, 263–269.
22. Jiang, Y.H. and Ehlers, M.D. (2013) Modeling autism by SHANK gene mutations in mice. *Neuron*, **78**, 8–27.
23. Lyst, M.J. and Bird, A. (2015) Rett syndrome: a complex disorder with simple roots. *Nat. Rev. Genet.*, **16**, 261–274.
24. Guy, J., Gan, J., Selfridge, J., Cobb, S. and Bird, A. (2007) Reversal of neurological defects in a mouse model of Rett syndrome. *Science*, **315**, 1143–1147.
25. Lioy, D.T., Garg, S.K., Monaghan, C.E., Raber, J., Foust, K.D., Kaspar, B.K., Hirrlinger, P.G., Kirchhoff, F., Bissonnette, J.M., Ballas, N. *et al.* (2011) A role for glia in the progression of Rett's syndrome. *Nature*, **475**, 497–500.
26. Yin, J. and Yuan, Q. (2014) Structural homeostasis in the nervous system: a balancing act for wiring plasticity and stability. *Front. Cell. Neurosci.*, **8**, 439.
27. Ballas, N., Lioy, D.T., Grunseich, C. and Mandel, G. (2009) Non-cell autonomous influence of MeCP2-deficient glia on neuronal dendritic morphology. *Nat. Neurosci.*, **12**, 311–317.
28. Nguyen, M.V., Felice, C.A., Du, F., Covey, M.V., Robinson, J.K., Mandel, G. and Ballas, N. (2013) Oligodendrocyte lineage cells contribute unique features to Rett syndrome neuropathology. *J. Neurosci.*, **33**, 18764–18774.
29. Derecki, N.C., Cronk, J.C., Lu, Z., Xu, E., Abbott, S.B., Guyenet, P. G. and Kipnis, J. (2012) Wild-type microglia arrest pathology in a mouse model of Rett syndrome. *Nature*, **484**, 105–109.
30. Maezawa, I. and Jin, L.W. (2010) Rett syndrome microglia damage dendrites and synapses by the elevated release of glutamate. *J. Neurosci.*, **30**, 5346–5356.
31. Bolton, M.M. and Eroglu, C. (2009) Look who is weaving the neural web: glial control of synapse formation. *Curr. Opin. Neurobiol.*, **19**, 491–497.